

# A polarized synchrotron template for CMBP experiments after WMAP data

G. Bernardi<sup>1,2,3</sup>, E. Carretti<sup>1</sup>, R. Fabbri<sup>4</sup>, C. Sbarra<sup>1</sup>, S. Poppi<sup>5</sup>, S. Cortiglioni<sup>1</sup>, J.L. Jonas<sup>6</sup>

<sup>1</sup>*I.A.S.F./C.N.R. Bologna, Via Gobetti 101, I-40129 Bologna, Italy*

<sup>2</sup>*Dipartimento di Astronomia, Università degli Studi di Bologna, Via Ranzani 1, I-40127 Bologna, Italy*

<sup>3</sup>*ATNF/CSIRO, P.O. BOX 76, EPPING, NSW, 1710, Australia*

<sup>4</sup>*Dipartimento di Fisica, Università di Firenze, Via Sansone 1, I-50019 Sesto Fiorentino (FI), Italy*

<sup>5</sup>*I.R.A./C.N.R. Bologna, Via Gobetti 101, I-40129 Bologna, Italy*

<sup>6</sup>*Department of Physics & Electronics, Rhodes University, PO Box 94, Grahamstown 6140, South Africa*

Accepted. Received; in original form

## ABSTRACT

We build template maps for the polarized Galactic-synchrotron emission on large angular scales (FWHM = 7°), in the 20-90 GHz microwave range, by using WMAP data. The method, presented in a recent work, requires a synchrotron total intensity survey and the *polarization horizon* to model the polarized intensity and a starlight polarization map to model polarization angles. The basic template is obtained directly at 23 GHz with about 94% sky-coverage by using the synchrotron map released by the WMAP team. Extrapolations to 32, 60 and 90 GHz are performed by computing a synchrotron spectral index map, which strongly reduces previous uncertainties in passing from low (1.4 GHz) to microwave frequencies. Differing from low frequency data, none of our templates presents relevant structures out of the Galactic Plane. Our map at 90 GHz suggests that the synchrotron emission at high Galactic latitudes is low enough to allow a robust detection of the *E*-mode component of the cosmological signal on large-scale, even in models with low-reionization ( $\tau = 0.05$ ). Detection of the weaker *B*-mode on the largest scales ( $\ell < 10$ ) might be jeopardized unless the value  $\tau = 0.17$  found by WMAP is confirmed, and  $T/S > 0.1$ . For lower levels of the gravitational-wave background the *B*-mode seems to be accessible only at the  $\ell \sim 100$  peak and in selected low-synchrotron emission areas.

**Key words:** polarization, Galaxy, cosmic microwave background, Method: numerical.

## 1 INTRODUCTION

Recent results by DASI (Kovac et al. 2002) and WMAP (Bennett et al 2003a) have opened a new window in studying both the Cosmic Microwave Background (CMB) and the Galaxy.

The polarized signal detected with the DASI experiment, as well as the WMAP measurement of the temperature-polarization cross-spectrum  $C_\ell^{TE}$ , emphasized the importance of studying CMB Polarization (CMBP). In particular, the discovery of a relevant signal on large angular scales performed by WMAP has provided evidence of an unexpectedly early reionization era (Kogut et al. 2003).

Furthermore, WMAP provided the first all-sky total-intensity maps of the microwave Galactic emission, allowing an insight into synchrotron, dust and free-free components of the Galaxy (Bennett et al. 2003b).

A sound measurement of CMBP requires good knowledge of polarized foregrounds (both Galactic and extragalactic), which are potentially more dangerous than in total intensity. This is even more true for the *B*-mode, retaining information on the gravitational-wave background (Kamionkowski & Kosowski, 1998), whose emission level is expected to be orders of magnitude below that of the *E*-mode.

Among all foreground components, the Galactic synchrotron radiation is expected to be the most relevant up to 100 GHz. The lack of data in both the CMB frequency range and at high Galactic latitudes makes the building of templates necessary (Kogut & Hinshaw 2000, Giardino et al. 2002, Bernardi et al. 2003a, hereafter B03). These can substantially help in studying how to extract CMB maps from contaminated signals (e.g. see Bennett et al. 2003b).

In B03 we presented a method modelling the Galactic polarized-synchrotron emission by using the radio-continuum total intensity surveys available at low frequency ( $< 1.4$  GHz) to model the polarized intensity, and starlight polarization optical data as a template for polarization angles.

Template maps obtained with this method are virtually free of Faraday rotation. However, when extrapolating low frequency data (the only available before the latest WMAP release) to the cosmological window, uncertainties arise on the spectral index to be used. In B03 we used the mean spectral index derived by Platania et al. (1998) up to 19 GHz, since no information were available at higher frequencies. In addition, variations across the sky were too poorly known to be taken into account.

The WMAP release of total-intensity synchrotron maps in the cosmological window gives us the possibility to significantly improve our templates. Actually, the application of our method directly at frequencies of interest for CMBP fully avoids extrapolation uncertainties.

Our templates are built with  $\text{FWHM} = 7^\circ$  at the three frequencies of 23, 32 and 90 GHz interesting for the SPoRT experiment (Cortiglioni et al. 2004), one of whose aims is studying the CMBP foregrounds. We also generate a template at 60 GHz, this frequency being of interest for other CMB experiments (WMAP, Planck). All of the templates cover large fractions of the sky, namely 94% at 23 GHz and 92% at 32, 60 and 90 GHz. In addition, we calculate polarized-synchrotron angular power spectra both for the full-sky templates and for the high Galactic latitude emission, discussing possible effects on the measurement of CMBP  $E$  and  $B$ -mode spectra.

The paper is organized as follows: in Section 2 we apply our method to WMAP data at 23 GHz and provide a Galactic polarized synchrotron template at the same frequency; in Section 3 we extrapolate our results up to 90 GHz; in Section 4 we describe the angular power spectra of our full-sky templates at the different frequencies, in Section 5 we compute the angular power spectra for the high Galactic latitude emission and compare synchrotron to CMBP and, finally, conclusions are presented in Section 6.

## 2 A POLARIZED TEMPLATE AT 23 GHZ USING WMAP DATA

In B03 we presented a method to obtain a template for the polarized Galactic synchrotron emission based on total intensity radio maps, starlight polarization data and the modelization of a *polarization horizon* as suggested by several authors (Duncan et al. 1997, Gaensler et al. 2001, Landecker et al. 2002).

The method is based on separate derivations of the polarized intensity and polarization angle maps. Whereas the latter is obtained from starlight polarization data, the former is the result of the application to total-intensity synchrotron maps of a filter mimicking the effects of the polarization horizon.

The main steps of our method can be summarized as follows:

- (i) a total intensity synchrotron map is obtained from

available surveys, after separating the CMB and free-free components when necessary;

- (ii) a filter accounting for the effects of the polarization horizon is applied to the  $I$  map, providing the polarized intensity  $I_p = \sqrt{Q^2 + U^2}$ ;

- (iii) a polarization-angle map is obtained from starlight data by interpolating the non-uniform data coverage;

- (iv) the polarized-intensity and polarization-angle maps are used to compute  $Q$  and  $U$  templates including a convolution with a  $\text{FWHM} = 7^\circ$  Gaussian filter to match the SPoRT angular resolution (finer resolutions are not possible due to the sampling of starlight polarization data).

Before WMAP, total intensity surveys were available up to 1.4 GHz and our templates were limited by our ignorance of the spectral index distribution needed to extrapolate to higher frequencies. Indeed, previous templates at 22, 32, 60 and 90 GHz were obtained by using a constant spectral index  $\beta = -3$ , corresponding to the mean value between 1.4 and 19 GHz (Platania et al. 1998).

The model is now substantially improved by using the latest WMAP data, including a total-intensity synchrotron map (cleaned from CMB, free-free and dust contributions) with resolution of  $1^\circ$  at 23 GHz, that directly allows us to compute the template at a frequency interesting for CMBP purposes.

The polarized intensity map is obtained by applying to the 23 GHz synchrotron map the equation

$$I_p(\nu, l, b) = p \frac{R_{ph}}{L(l, b)} I(\nu, l, b) \quad (1)$$

mimicking the polarization horizon effects (see B03). Here  $I_p$  and  $I$  are the polarized and total intensity of the synchrotron radiation, respectively,  $L(l, b)$  is the thickness of the synchrotron emitting region,  $p$  is the polarization degree,  $R_{ph}$  is the distance of the polarization horizon. We adopt the same normalization factor  $p R_{ph} = 0.9$  Kpc as computed in B03.

From this polarized brightness temperature, and using the same polarization-angle map as in B03,  $Q$ ,  $U$  and  $I_p$  maps are obtained. They are shown in Figure 1, where the grey region corresponding to the North Celestial Pole is an area where the interpolation of starlight polarization angles failed (see B03 for details). It is worth emphasizing that the new maps cover almost 94% of the sky, to be compared with the half-sky coverage of the B03 template.

Confirming the B03 results, the distribution of the polarized intensity is quite different from that of total intensity (Figure 2). The latter peaks towards the Galactic centre and traces well the Galactic Plane. Instead, the polarized emission has a sub-dominant Galactic Centre and the Galactic Plane shows a patchy structure (Figure 3).

A comparison with the B03 template shows a general agreement between the two maps along the Galactic Plane, and in particular in the following three regions:

- (i) *Fan region* located at  $100^\circ \leq l \leq 160^\circ$ ;
- (ii) the region at  $30^\circ \leq l \leq 45^\circ$ ;
- (iii) the region around  $l \simeq 15^\circ$ , though only partially present in the B03 template.

A comparison with the Parkes survey (Figure 4) shows remarkable similarities as well. The brightest polarized region in our template is at Galactic longitude  $315^\circ \leq l \leq 345^\circ$ ,

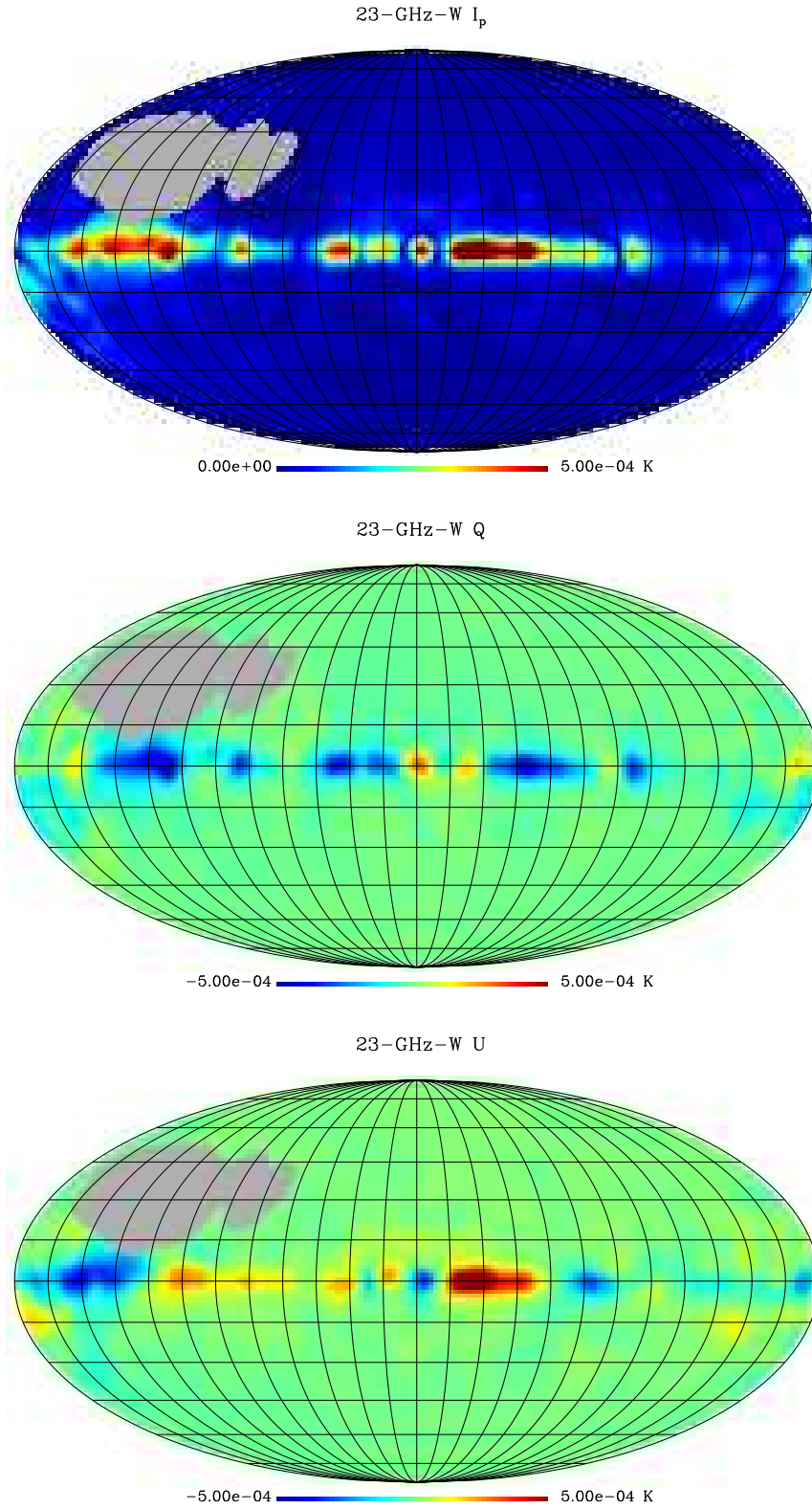


**Figure 1.** Our 23 GHz polarized synchrotron template obtained using WMAP data as total intensity emission. Maps are convolved with a  $FWHM = 7^\circ$  Gaussian filter.

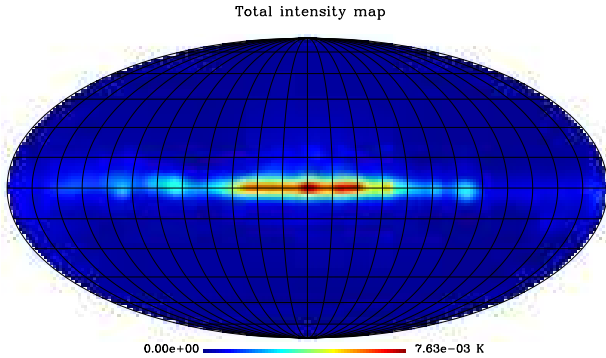


**Figure 2.** WMAP's total intensity synchrotron emission at 23 GHz (from Bennett et al. 2003b) smoothed with a  $7^\circ$  beam.

where also Duncan et al. (1997) found a high level in the polarized background at 2.4 GHz (see also Figure 4). The bright features present in our template correspond to emission spots in the Duncan map, with the exception of the large region centred at  $l \sim 300^\circ$ . This discrepancy is the same noted in B03 and is not surprising. Actually, this is a peculiar area with strong variations in Rotation Measures (Sofue & Fujimoto 1983, Duncan et al. 1997, B03), so that the absence of polarized emission in the Parkes data is likely to be due to Faraday depolarization.

Out of the Galactic Plane, the model computed with the WMAP data (hereafter the 23-GHz-W template) does not show any relevant structure. This differs from the emission at 1.4 GHz, where the Northern Galactic Spur is among the main polarized structures, both in the Brouw & Spoelstra (1976) data and our 1.4 GHz B03 model. The situation is similar in the total-intensity case, where the Northern Galactic Spur is a prominent feature at 1.4 GHz, but is no more significant at 23 GHz. This behaviour could be explained following Bennett et al. (2003b), who showed that the spectral index of the synchrotron radiation in the 0.408–23 GHz range is quite different in the Plane and out of it. The Galactic Plane having a flatter spectral index becomes more and more dominant with increasing frequency.

### 3 SPECTRAL INDEX BEHAVIOUR AND EXTRAPOLATION TO HIGHER FREQUENCIES

The most important frequency range for CMBP studies is around 90 GHz, where the polarized foregrounds are expected to have minimum emission. Since the 94 GHz synchrotron map provided by WMAP appears to be dominated by noise at high Galactic latitudes, we do not apply our method directly to it to provide a synchrotron template at 90 GHz. Instead, we prefer to extrapolate our 23 GHz template, characterised by a better  $S/N$  ratio.

Faraday rotation effects are negligible at frequencies higher than 20 GHz (e.g. see B03). In absence of RM modulation, polarization and total intensity are expected to have the same behaviour.

Synchrotron spectral-index variations across the sky have to be carefully modelled when extrapolating synchrotron

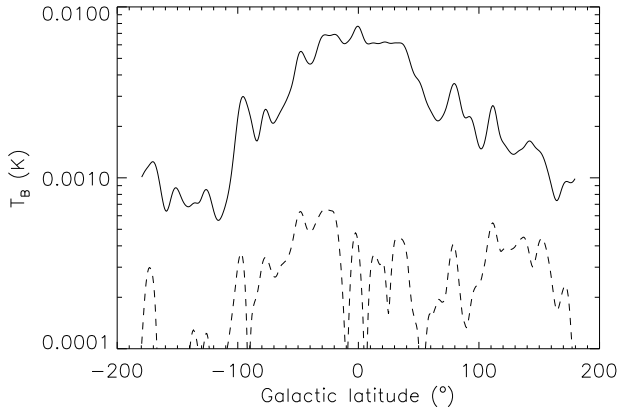


**Figure 3.** Comparison between the total (observed, solid line) and polarized (template, dashed line) brightness temperatures along the Galactic Plane at 23 GHz. We consider all the pixels with  $|b| \leq 0.1^\circ$

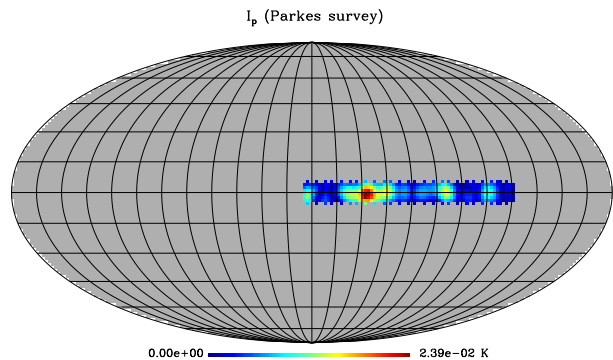


**Figure 4.** Polarized intensity emission from the Parkes survey at 2.4 GHz smoothed on  $7^\circ$  (Duncan et al. 1997).

maps to higher frequencies. Bennett et al. (2003b) provided a spectral-index map, for the 0.408–23 GHz range, which applies to a mixture of synchrotron and free-free emissions and is not directly useful for our purposes.

We thus extract a nearly full-sky synchrotron map at 1.4 GHz, by means of a modified Dodelson technique (B03) to separate between components, from the Haslam et al. (1982) survey at 0.408 GHz, the Reich (1982) survey at 1.4 GHz, and the Jonas et al. (Jonas, Baart & Nicolson, 1998) survey at 2.3 GHz.

Properties of data at 0.408 GHz and 1.4 GHz have already been described in B03 (and references therein). Data at 2.3 GHz correspond to a radio-continuum survey of the Southern sky ( $-83^\circ < \delta < 13^\circ$ ), with angular resolution of 20 arcmin.

All maps are smoothed to the same resolution of 51 arcmin, corresponding to data at 0.408 GHz. The free-free subtraction is performed adopting the B03 model for the spatial distribution of the synchrotron spectral index which, being symmetric with respect to both the Galactic Plane

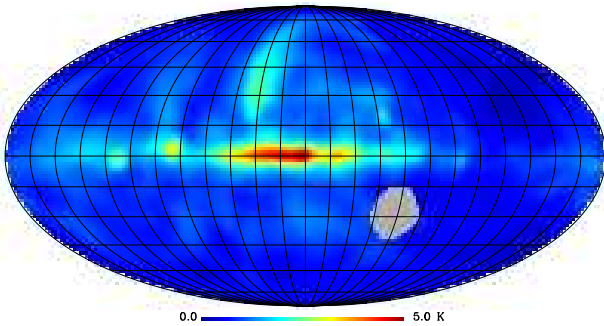


**Figure 5.** Total intensity synchrotron map at 1.4 GHz on  $7^\circ$  (cleaned from free-free contribution) obtained from Haslam et al. (1982), Reich (1982) and Jonas et al. (1998) maps.

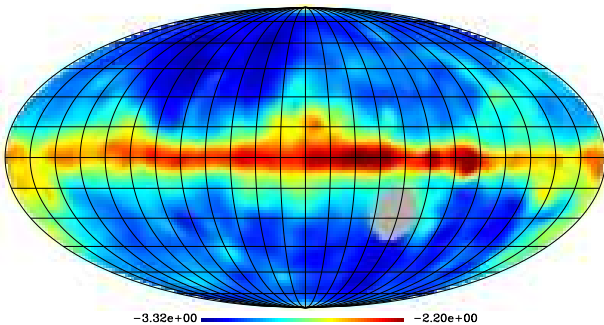


**Figure 6.** Spectral index map of the synchrotron emission on  $7^\circ$  angular scales between 1.4 and 23 GHz. The grey region around the South Celestial Pole is the unobserved area in the 2.3 GHz survey.

and the Galactic centre, can be extended to the Southern sky.

Due to different sky coverages of the available surveys, synchrotron maps are built separately in the Northern and in the Southern hemispheres. Where the two maps overlap, we retain information from the Northern one, since the zero level of its parent surveys are more accurately determined than that at 2.3 GHz. Moreover, we correct the offset of the Southern synchrotron map shifting its mean level to the that of the Northern map in the overlapping region. Discontinuities at borders are at negligible levels for our purposes, being cancelled out by the convolution with a FWHM =  $7^\circ$  Gaussian filter. The final map, covering almost 99% of the sky, is shown in Figure 5.

A comparison with the 23 GHz synchrotron map provided by WMAP allows us to determine the synchrotron spectral index in the 1.4–23 GHz range (Figure 6).

The overall pattern of our synchrotron spectral-index map is substantially in agreement with that by Bennett et al. (2003b): the spectral index is rather flat along the Galactic Plane, whereas steeper spectra are found at high Galactic latitudes. As shown in Fig.7, the typical spectral index is

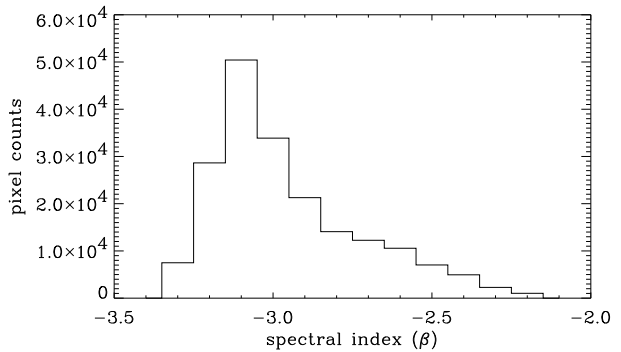


**Figure 7.** Synchrotron spectral index distribution between 1.4 and 23 GHz.

$\beta = -3.1$ , which is steeper than the value found by Bennett et al. (2003b); this might be due to the thermal contribution in their data.

We use our spectral-index map to extrapolate the 1.4 GHz B03 template up to 23 GHz (hereafter the 23-GHz-LF [low frequency] template). The result is shown in Figure 8, and can be compared with the 23-GHz-W map to further test our template-building procedure.

A general agreement in the morphology can be observed. In particular, the most relevant characteristic in both maps is the lack of features at high Galactic latitudes. The Northern Galactic Spur, present at 1.4 GHz, disappears when extrapolated with the spectral-index map of Figure 6, in agreement with 23-GHz-W. Also the main features in the Galactic Plane are similar.

Indeed, the model applied to the 0.408–1.4 GHz data (including the free-free component separation) and extrapolated to 23 GHz by using spatially varying spectral indices presents results very similar to the 23-GHz-W template, which is free from extrapolation uncertainties.

In order to produce template maps up to 90 GHz, the spectral index map in Figure 6 is not sufficient. A steepening at higher frequencies, in fact, has been found by Bennett et al. (2003b), who reported a mean steepening of 0.5 in the 23–41 GHz range. To extrapolate our 23-GHz-W template, thus, we increase the spectral indexes by this amount.

Figure 9 shows  $I_p$ ,  $Q$  and  $U$  maps at 90 GHz, which is the most interesting frequency for CMB measurements. Maps at 32 and 60 GHz look qualitatively rather similar. As already pointed out in this section, the flatter Galactic Plane component becomes more and more dominant with increasing frequency. A further important characteristic is that the Galactic Plane essentially retains its morphology. However, again due to the different spectral behaviour, the *Fan region* is fainter and fainter with increasing frequency respect with the  $300^\circ < l < 330^\circ$  region.

#### 4 ANGULAR PROPERTIES OF THE POLARIZED TEMPLATE

The distribution of the polarized emission at different angular scales is described by the angular power spectra (APS)  $C_\ell^E$ ,  $C_\ell^B$  and  $C_\ell^P = C_\ell^E + C_\ell^B$ . We compute them by the

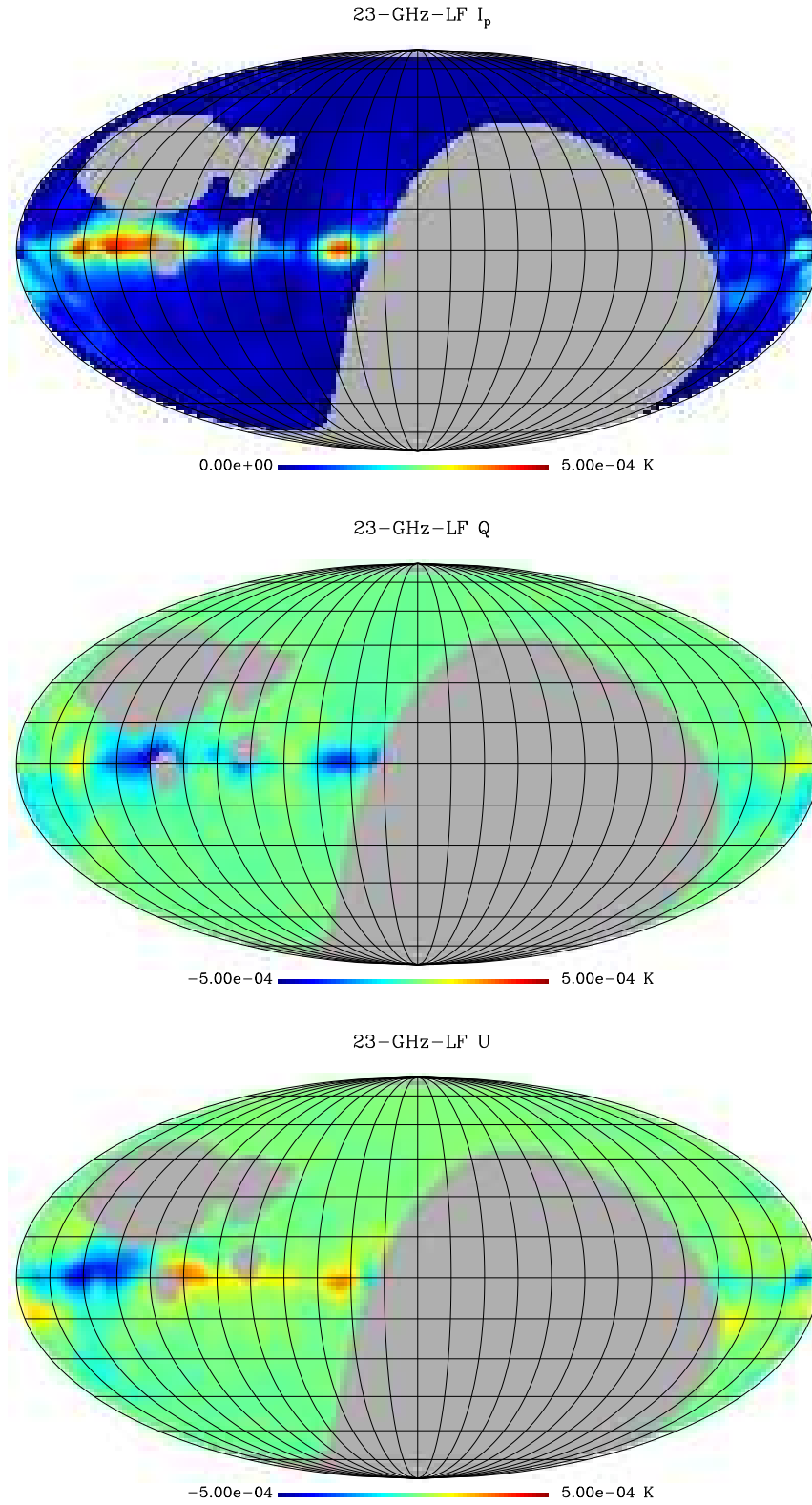


**Figure 8.** Maps of our template obtained from the 1.4 GHz B03 one scaled to 23 GHz (23-GHz-LF). The angular resolution is  $7^\circ$ .



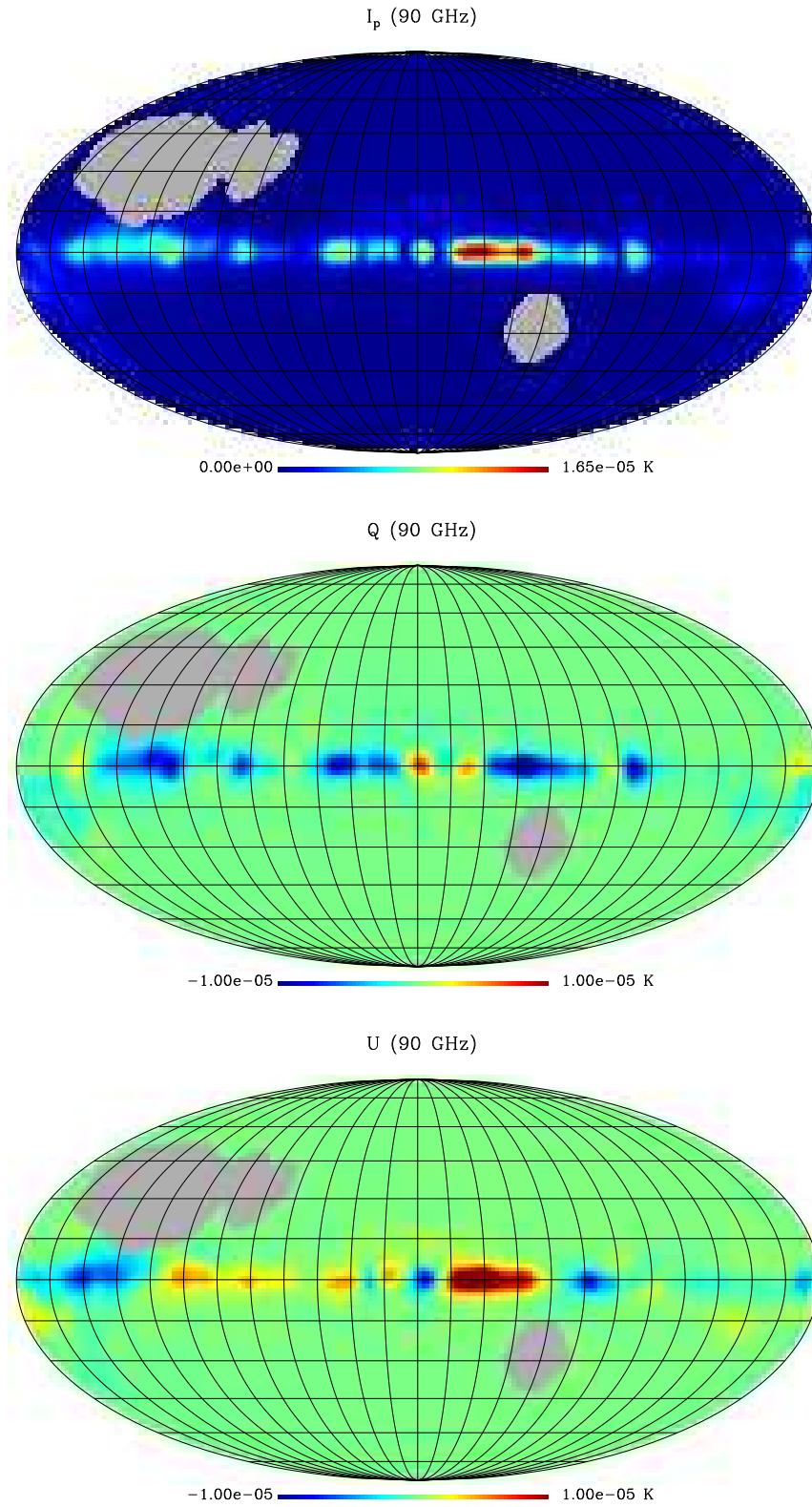


**Figure 9.** Maps of our template at 90 GHz. The angular resolution is  $7^\circ$ .

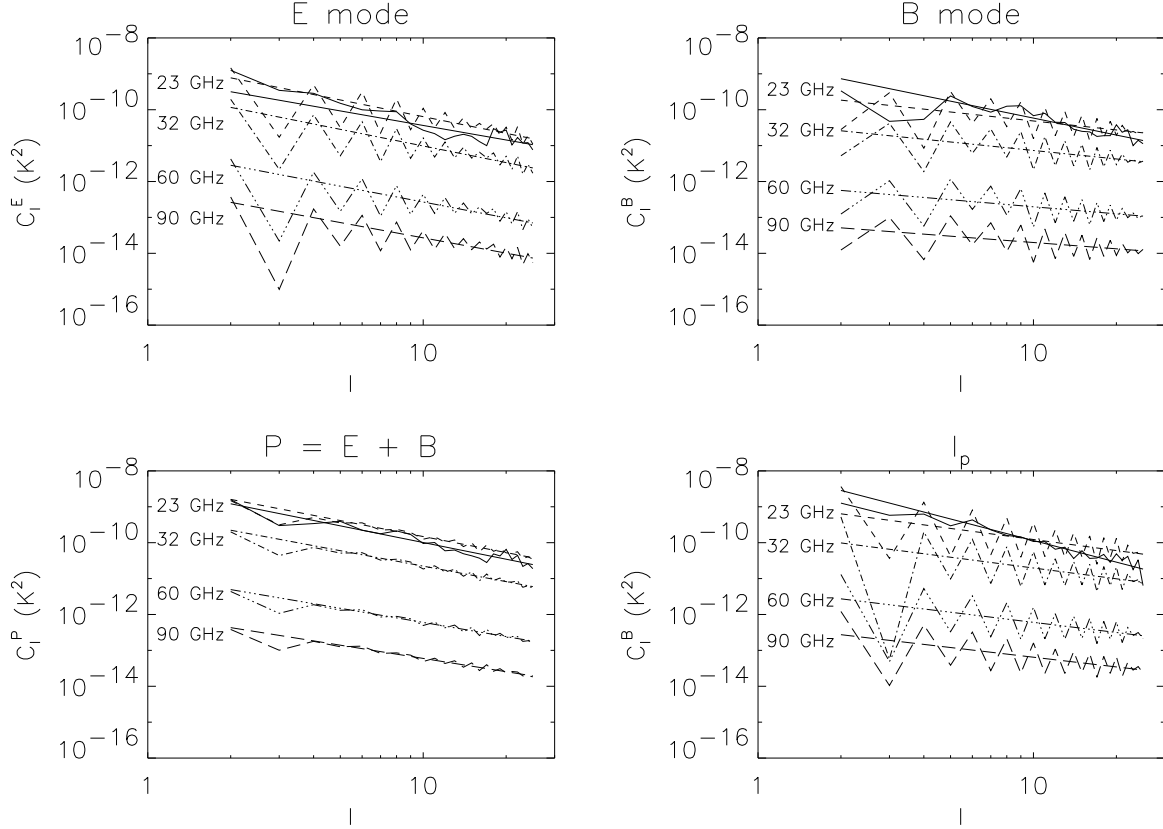


**Figure 10.**  $C_\ell^E$ ,  $C_\ell^B$ ,  $C_\ell^P$  and  $C_\ell^{I_p}$  spectra computed for the 23-GHz-LF (solid) and 23-GHz-W templates (dotted). Spectra for the 32 (dashed), 60 (dashed-dotted) and 90 GHz (dashed-triple dotted) models are shown as well.

**Table 1.** Best fit APS slopes and amplitudes as obtained from our templates in the  $2 \leq \ell \leq 25$  range using WMAP data. First and second lines report the 23-GHz-LF and 23-GHz-W templates respectively.

$\nu$ (GHz)	$\alpha_E$	$C_{10}^E$ ( $\mu\text{K}^2$ )	$\alpha_B$	$C_{10}^B$ ( $\mu\text{K}^2$ )	$\alpha_P$	$C_{10}^P$ ( $\mu\text{K}^2$ )	$\alpha_{I_p}$	$C_{10}^{I_p}$ ( $\mu\text{K}^2$ )
23-LF	$1.34 \pm 0.09$	$37 \pm 2$	$1.57 \pm 0.09$	$58 \pm 4$	$1.54 \pm 0.09$	$101 \pm 6$	$2.00 \pm 0.09$	$115 \pm 7$
23-W	$1.55 \pm 0.09$	$64 \pm 4$	$0.83 \pm 0.09$	$49 \pm 3$	$1.48 \pm 0.09$	$148 \pm 9$	$1.00 \pm 0.09$	$123 \pm 8$
32	$1.54 \pm 0.09$	$9.7 \pm 0.6$	$0.79 \pm 0.09$	$7.3 \pm 0.4$	$1.43 \pm 0.09$	$22 \pm 1$	$1.00 \pm 0.09$	$20 \pm 1$
60	$1.47 \pm 0.09$	$0.27 \pm 0.02$	$0.65 \pm 0.09$	$0.20 \pm 0.01$	$1.31 \pm 0.09$	$0.60 \pm 0.04$	$0.94 \pm 0.09$	$0.60 \pm 0.04$
90	$1.41 \pm 0.09$	$(27 \pm 2) \times 10^{-3}$	$0.58 \pm 0.09$	$(20 \pm 1) \times 10^{-3}$	$1.23 \pm 0.09$	$(60 \pm 4) \times 10^{-3}$	$0.90 \pm 0.09$	$(65 \pm 4) \times 10^{-3}$

correlation-function method (see Sbarra et al. 2003 for details), accounting for irregularities in the sky coverage. The APS of our templates are reported in Figure 10. Their overall behaviour, with particular reference to  $C_\ell^P$ , can be represented by a power law:

$$C_\ell^Y = C_{10}^Y \left( \frac{\ell}{10} \right)^{-\alpha_Y} \quad Y = E, B, P, I_p, \quad (2)$$

whose best fit parameters in the  $2 \leq \ell \leq 25$  range are reported in Table 1. We perform a linear fit to the quantities  $\log C_\ell$  and  $\log \ell$  giving greater weights to high order multipoles (since  $C_\ell$  is an average of  $(2\ell + 1)$  squared harmonic amplitudes). In addition, we compute the scalar spectrum  $C_\ell^{I_p}$  of  $I_p$  for comparison with other works.

The two templates at 23 GHz are in good agreement in the overall intensity, whereas the slopes are somewhat different, the 23-GHz-W  $C_\ell^B$  being flatter even if the slopes of the total polarization spectrum  $C_\ell^P$  are statistically equal. Differences might be due to the different sky coverages of the two maps. In fact, we have computed the APS for the 23-GHz-W template limited to the coverage of 23-GHz-LF and have found a better agreement between the two templates. This suggests the Southern sky contributes to make the overall slope flatter.

A slight decrement of the slopes with increasing frequencies appears in the  $C_\ell^B$  and  $C_\ell^P$  spectra of our templates, the 90 GHz ones being the flattest. However, these



variations are within  $2\sigma$  of the slopes themselves and a robust result cannot be claimed.

While the slopes of  $C_\ell^E$  and  $C_\ell^P$  are compatible with each other,  $C_\ell^B$  and  $C_\ell^{I_p}$  are significantly flatter and this behaviour is still not clear. In addition,  $C_\ell^E$  and  $C_\ell^P$  slopes are in agreement with those previously calculated in real radio surveys (Tucci et al. 2000, Baccigalupi et al. 2001, Bruscoli et al. 2002, Giardino et al. 2002). However, one should take into account that a perfect agreement is not expected at all, since our template and previous works differ in both the angular scale and the frequency (1.4–2.7 GHz for the real surveys).

## 5 HIGH GALACTIC LATITUDE EMISSION

The templates presented here predict that the synchrotron polarized emission is concentrated on the Galactic Plane. As it already occurs for the total intensity, this suggests us to search for the CMBP signal at high Galactic latitude.

Let's us recall that this was not that obvious before the present work, since large and bright features exist, out of the Galactic Plane, in low frequency observations (see, for example, the Northern Galactic Spur in the 1.4 GHz polarized data of Brouw & Spoelstra 1976).

To study the expected synchrotron emission at high Galactic latitudes we mask off the Galactic Plane by using the pixel-count histogram of the  $I_p$  map at 23 GHz shown in Figure 11, in a way similar to that described by Bennett et al. (2003b). The intensity distribution is strongly asymmetric, and pixels with the higher values correspond to the Galactic Plane emission to be cut away. To set the value of the threshold defining which pixels are to be discarded, we fit the peak of the distribution and subtract the best-fit curve from the histogram. The peak of the residual distribution was chosen by Bennett et al. (2003b) as the threshold value.

Differing from the Gaussian behaviour followed by temperature data (Bennett et al. 2003b), the low emission part of the polarized intensity  $I_p = \sqrt{Q^2 + U^2}$  is better represented by a Rayleigh distribution, as it would be if  $Q$  and  $U$  were gaussian distributed:

$$F(I_p) = A I_p e^{-I_p^2/(2\sigma^2)} \quad (3)$$

where  $A$  and  $\sigma$  are parameters to be determined.

We fit the distribution in the 0–22  $\mu\text{K}$  range. The best-fit subtracted histogram has a peak at 39.1  $\mu\text{K}$ ; however, we prefer to be more conservative and set the threshold at 34.1  $\mu\text{K}$  of the secondary peak. The pixel mask of the retained pixels ( $I_p < 34.1 \mu\text{K}$ ) covers about 68% of the sky and is shown in Figure 12.

APS computed on our template maps after applying this mask are shown in Figure 13. Power spectra at high Galactic latitudes can be represented by power laws apart from the region at large  $\ell$ , where they are observed to flatten, probably due to pixel noise. Therefore, we fit the  $2 < \ell < 15$  range and report the results in Table 2.

At each frequency, power spectra levels are about two orders of magnitude below those including the Galactic Plane which, therefore, dominates the APS calculated in Section 4.

Slopes are steeper than those computed on the overall

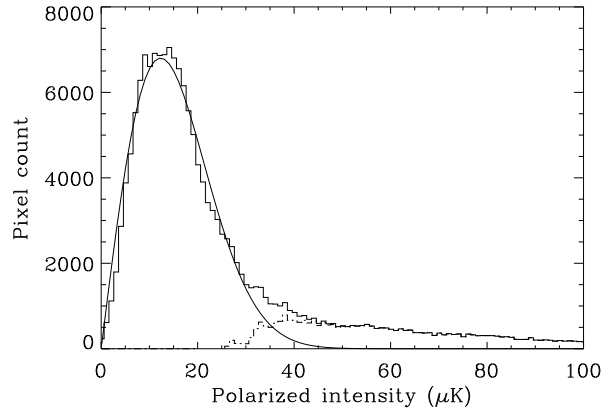


**Figure 11.** Histogram of the polarized intensity distribution in the 23-GHz-W template. The solid curve represents the Rayleigh function used to fit the distribution and the dashed line represents the residual distribution.

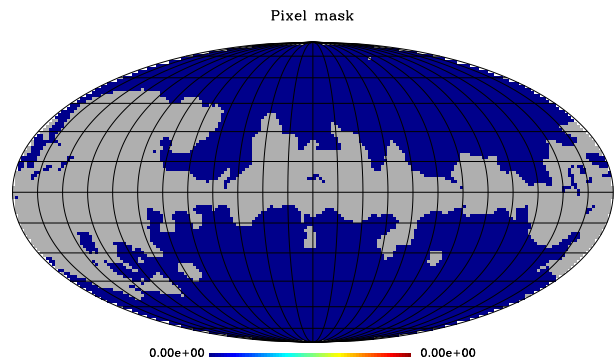


**Figure 12.** The pixel mask in Mollweide projection. Grey pixels represent the excluded region.

templates, in particular for  $C_\ell^B$ , suggesting that the flattening observed in the full-sky templates is mainly due to Galactic Plane features. No significant flattening with increasing frequency is found at high Galactic latitude.

Figure 14 shows a comparison between our estimate of synchrotron power spectra at high Galactic latitudes and expected CMBP angular spectra. The power spectra of our templates are converted to CMB thermodynamic temperature by multiplying them by the square of the conversion factor

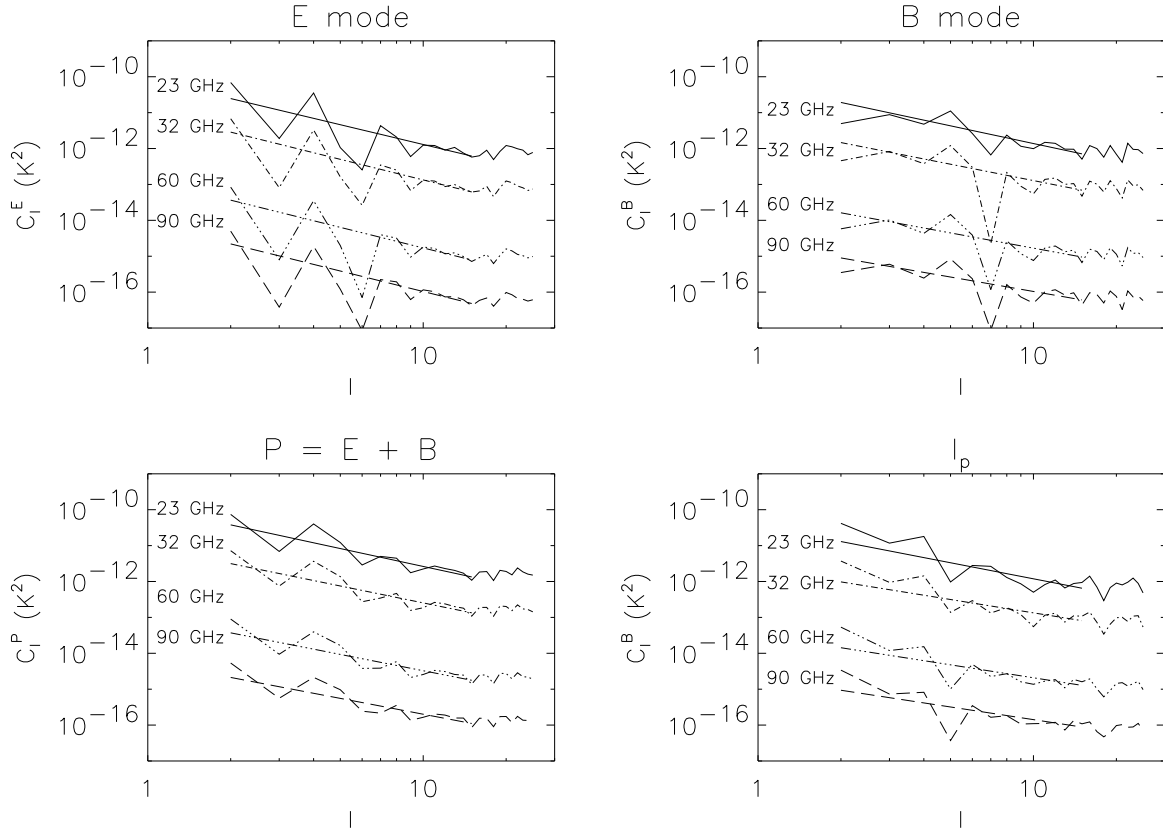
$$c = \left( \frac{2 \sinh \frac{x}{2}}{x} \right)^2 \quad (4)$$

where  $x \equiv h\nu/kT_{cmb} \approx \nu/56.8 \text{ GHz}$ . CMBP angular spectra are computed assuming cosmological-parameter values as in the *concordance model* determined by WMAP data (Spergel et al. 2003):  $h_0 = 71$ ,  $\Omega_b = 0.044$ ,  $\Omega_{CDM} = 0.226$ ,  $\Omega_\Lambda = 0.73$ ,  $\tau = 0.17$  and initial adiabatic fluctuations.

Our templates suggest that at 90 GHz CMBP *E*-mode measurements in the  $2 < \ell < 20$  multipole range should be only marginally contaminated by synchrotron polarized

**Table 2.** Best fit APS slopes and amplitudes as obtained from our templates in the  $2 \leq \ell \leq 15$  range after the pixel mask is applied.

$\nu$ (GHz)	$\alpha_E$	$C_{10}^E$ ( $\mu\text{K}^2$ )	$\alpha_B$	$C_{10}^B$ ( $\mu\text{K}^2$ )	$\alpha_P$	$C_{10}^P$ ( $\mu\text{K}^2$ )	$\alpha_{I_p}$	$C_{10}^{I_p}$ ( $\mu\text{K}^2$ )
23	$1.8 \pm 0.2$	$1.3 \pm 0.1$	$1.6 \pm 0.2$	$1.4 \pm 0.1$	$1.7 \pm 0.2$	$2.6 \pm 0.2$	$1.5 \pm 0.2$	$1.2 \pm 0.1$
32	$1.9 \pm 0.2$	$0.13 \pm 0.01$	$1.5 \pm 0.2$	$0.13 \pm 0.01$	$1.6 \pm 0.2$	$0.25 \pm 0.02$	$1.2 \pm 0.2$	$0.13 \pm 0.02$
60	$1.9 \pm 0.2$	$(1.7 \pm 0.1) \times 10^{-3}$	$1.4 \pm 0.2$	$(1.7 \pm 0.1) \times 10^{-3}$	$1.5 \pm 0.2$	$(3.3 \pm 0.2) \times 10^{-3}$	$1.2 \pm 0.2$	$(2.1 \pm 0.1) \times 10^{-3}$
90	$1.9 \pm 0.2$	$(1.04 \pm 0.07) \times 10^{-4}$	$1.3 \pm 0.2$	$(1.04 \pm 0.07) \times 10^{-4}$	$1.5 \pm 0.2$	$(2.0 \pm 0.1) \times 10^{-4}$	$1.2 \pm 0.2$	$(1.4 \pm 0.1) \times 10^{-4}$

**Figure 13.**  $C_\ell^E$ ,  $C_\ell^B$ ,  $C_\ell^P$  and  $C_\ell^{I_p}$  spectra computed for the 23 GHz template with the high Galactic latitude mask applied (dotted line). Spectra for the 32 (dashed), 60 (dashed-dotted) and 90 GHz (dashed-triple dotted) models are shown as well.

radiation. Furthermore, even a less reionized Universe ( $\tau = 0.05$ ) should be accessible at this frequency.

It is worth noticing that even relaxing our hypotheses of a steepening by 0.5 in the spectral indexes between 23 and 90 GHz, e.g. simply adopting the spectral-index map of Figure 6, the normalization of the synchrotron power spectrum would be just a factor  $\sim 4$  higher, which does not substantially modify the conclusions drawn above. In fact, the CMBP power spectrum of models with  $\tau = 0.17$  and  $\tau = 0.05$  are about two and one orders of magnitude larger than the synchrotron spectrum, respectively.

Obtaining a clean measurement of the CMBP  $B$ -mode looks more difficult. Large values of the optical depth  $\tau$  push a large-scale peak at  $\ell < 10$  and open a second window to detect this faint signal beyond that at  $\ell \sim 100$  (Kamionkowski & Kosowsky 1998). Figure 14 shows two models with the

same cosmological parameters as above, but with the addition of a gravitational wave background with tensor to scalar fluctuation power ratio  $T/S = 0.1$  and  $T/S = 0.01$ , respectively. While the former looks reasonably free from synchrotron contamination, at least in the low multipole range ( $\ell < 10$ ), the level of the latter is comparable with our estimate of the synchrotron spectrum.

We can thus conclude that, for values  $\tau = 0.17$  and  $T/S > 0.1$ , a CMBP  $B$ -mode measurement on large angular scale free from synchrotron contamination is achievable. For lower  $T/S$  values, instead, detection of the  $B$ -mode would be only possible in selected regions with low foreground emission, and large enough to access the  $\ell \sim 100$  peak. A good example is the patch observed by the BOOMERanG experiment and selected for BaR-SPOrt (Cortiglioni et al. 2003),

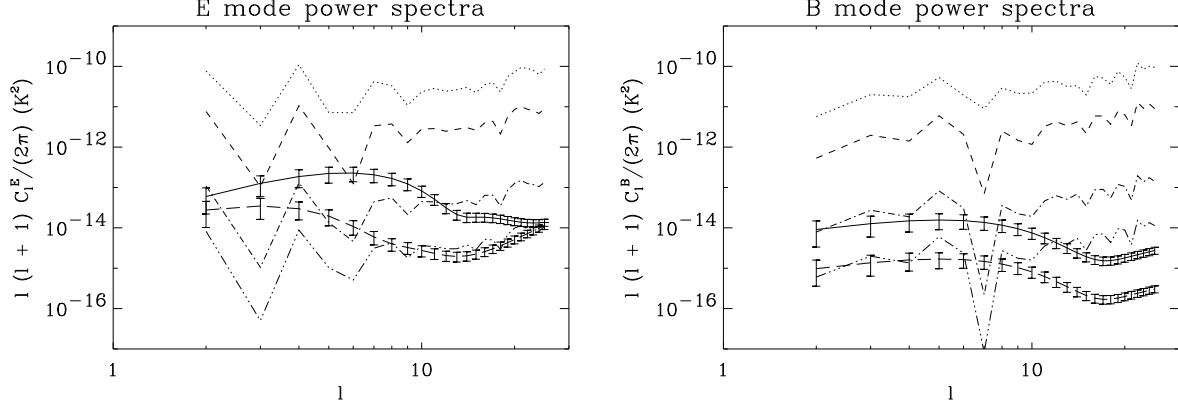


**Figure 14.** Left:  $C_\ell^E$  computed on the 23 GHz (dotted), 32 GHz (dashed), 60 GHz (dashed-dotted) and 90 GHz models (dashed-triple dotted). The solid and long-dashed lines represent the CMB  $E$ -mode spectrum of the *concordance model* with  $\tau = 0.17$  and  $\tau = 0.05$ , respectively. Errors represent the cosmic variance. Right: the same but for  $C_\ell^B$ . The solid and long-dashed lines represent CMB  $B$ -mode spectrum with  $T/S = 0.1$  and  $T/S = 0.01$ , respectively

**Table 3.**  $P_{\text{rms}}$  of our templates at the four reference frequencies in thermodynamic temperature. The  $P_{\text{rms}}$  is computed on the remaining 68% of the sky after applied the pixel mask. Bottom line reports the  $P_{\text{rms}}$  of the CMBP  $E$ -mode model with  $\tau = 0.17$ . The error on the CMBP  $P_{\text{rms}}$  takes into account only the cosmic variance contribution.

$\nu$ (GHz)	$P_{\text{rms}}$ ( $\mu\text{K}$ )
23	10
32	3.2
60	0.36
90	0.095
CMBP $E$ -mode ( $\tau = 0.17$ )	$0.49 \pm 0.03$
CMBP $E$ -mode ( $\tau = 0.05$ )	$0.189 \pm 0.007$

for which synchrotron contamination is expected to be under control already for  $T/S > 0.01$  (Bernardi et al. 2003b).

To complete our comparison between synchrotron and CMB, we compute the  $P_{\text{rms}}$  of our masked template maps at the four frequencies (Table 3) using the equation (Zaldarriaga 1998)

$$P_{\text{rms}} = \sqrt{\sum_{\ell} \frac{(2\ell+1)}{4\pi} (C_\ell^E + C_\ell^B) W_\ell} \quad (5)$$

where  $W_\ell$  is the window function defined as

$$W_\ell = e^{-\ell(\ell+1)\sigma^2} \quad (6)$$

and  $\sigma = \text{FWHM}/\sqrt{8 \ln 2}$

At 90 GHz, the  $P_{\text{rms}}$  signal is already lower than the value computed in B03 using the half faintest sky. Considering the 50% faintest sky, a  $P_{\text{rms}} \sim 0.057 \mu\text{K}$  is obtained with the present model, showing that the mean polarized value of the synchrotron background appears quite low in large part of the sky.

Table 3 shows that a  $\tau = 0.17$  model has a  $P_{\text{rms}}$  for the CMB  $E$ -mode which is about five times the  $P_{\text{rms}}$  of the high latitude synchrotron foreground. This suggests that even an

experiment having just the sensitivity to detect the  $P_{\text{rms}}$  has good chances to measure the optical depth  $\tau$ .

## 6 CONCLUSIONS

In this work we generate template maps of polarized Galactic synchrotron emission at 23, 32, 60 and 90 GHz using WMAP data.

We apply the method developed in B03 to the 23 GHz total intensity synchrotron map released by the WMAP team. This greatly improves the B03 templates avoiding the uncertainties in the extrapolation from low frequency. As for the previous work, the angular resolution is limited to  $\text{FWHM} = 7^\circ$  mainly due to the starlight polarization data sampling.

The basic template (23-GHz-W) is constructed at 23 GHz applying the method directly to the WMAP data and it covers almost all the sky (94%). Differing from the 1.4 GHz B03 template where the Northern Galactic Spur represents an important feature, 23-GHz-W does not present relevant structures out of the Galactic Plane. This replicates what already occurs in total intensity and leaves most part of the sky with low synchrotron emission and useful for CMBP investigations.

To achieve the templates at the other frequencies a spectral index map is required to extrapolate the 23-GHz-W result. Differing from Bennett et al. (2003b), which derived a spectral index map from 0.408 to 23 GHz with no free-free subtraction in the 0.408 GHz map, we computed the frequency behaviour using *pure* synchrotron maps at 1.4 and 23 GHz. The 23 GHz one is that released by the WMAP team. The 1.4 GHz map has been achieved from low frequency surveys by applying a Dodelson-like component separation. We use the Haslam et al. 0.408 GHz and the Reich 1.4 GHz surveys for the Northern sky and the Haslam et al. and the Jonas et al. 2.3 GHz ones for the Southern Hemisphere. The results is the first almost all-sky spectral index map of the Galactic synchrotron emission in the 1.4–23 GHz range. Furthermore, we add an extra 0.5 to the indices to

account for the steepening found by Bennett et al. (2003b) in the 23–41 GHz range and this spectral index map is used to compute template maps at 32, 60 and 90 GHz covering 92% of the sky.

The spectral index map provides steeper indexes at high Galactic latitudes so that the resulting templates have the Galactic Plane emission more and more dominant from 23 GHz up to 90 GHz. This difference also explains the disappearing of the Northern Galactic Spur in our templates. Unclear, instead, it is the reason for such a flat frequency spectrum found in the Galactic Plane, it being either intrinsic to the synchrotron emission (for instance due to a young population of relativistic electrons) or due to a residual thermal component.

Beyond the lack of relevant structures at high Galactic latitudes, the differences among the templates of this work and the B03 one also concern the APS. APS of our full-sky templates are dominated by the emission from the Galactic Plane and flatter slopes, namely in the 1.4–1.6 range for  $C_\ell^E$ , 0.5–0.8 for  $C_\ell^B$  and 1.2–1.5 for  $C_\ell^P$ . This general flattening is still not clear.

A further unclear point is that the synchrotron APS slopes (in particular  $C_\ell^B$  and  $C_\ell^P$ ) seem to flatten with increasing frequency. If confirmed, these two aspects would confirm that low frequency APS cannot be straightforwardly extrapolated from low to microwave frequencies.

The situation is less complex at high Galactic latitudes. In fact, limiting the analysis out of the Galactic Plane, a steepening of the slopes occurs, which become more similar to the B03 ones, and no significative dependency from the frequency is found.

Interesting conclusions are drawn by the comparison of the high Galactic latitude portion of our templates to CMBP as from the *concordance model* of the WMAP first-year data. Indeed, the CMBP *E*-mode spectrum is about 2 orders of magnitude above the synchrotron signal in our template at 90 GHz. Synchrotron is thus unlikely to contaminate the cosmological signal. Furthermore, even a less re-ionized Universe ( $\tau = 0.05$ ) should be dominant over the Galactic emission.

The situation looks different for the CMBP *B*-mode. Our template predicts that this cosmological signal might be accessible at largest scales ( $\ell < 10$ ) only for a Tensor to Scalar fluctuation power ratio  $T/S > 0.1$ . To investigate models with lower values of  $T/S$  one should restrict to selected low synchrotron emission areas large enough to detect the  $\ell \sim 100$  peak. An example is the sky patch observed by the BOOMERanG experiment where models with  $T/S > 0.01$  seem to be accessible (Bernardi et al. 2003b).

Our templates obviously rely on the assumption that WMAP's dust-correlated signal at 22 GHz is genuine synchrotron, as supported by Bennet et al. (2003b). However several authors (de Oliveira-Costa et al. 2003, Banday et al. 2003, Lagache 2003) recently support the opposite view, that WMAP's data may be more consistent with anomalous dust emission. For instance, while the spinning-dust model originally proposed by Draine & Lazarian (1998) may meet some difficulty, emission by very small grains is supported by Lagache (2003).

Considering that dust polarization level is likely less than 5% rather than the 15–30% of the synchrotron, a measurement of polarization at 22–32 GHz could help to decide

on this issue: should the polarization level be found a factor  $\sim 5$  below the predictions of our template, the role of anomalous dust emission would be supported.

Also, in such a case, the contamination of CMBP maps at 90 GHz would be even smaller than considered in our discussion above, and prospects for the detection of a cosmological B mode would be slightly better.

## ACKNOWLEDGMENTS

This work has been carried out in the frame of the SPOrt experiment, a programme funded by ASI. G.B. acknowledges a Ph.D. ASI grant. We thank an anonymous referee for useful comments. We acknowledge the use of CMBFAST package. Some of the results in this paper have been derived using the HEALPix<sup>\*</sup> (Gorski, Hivon, and Wandelt 1999) package. We acknowledge the use of the data<sup>†</sup> made publicly available by the WMAP team.

## REFERENCES

- Banday A.J., Dickinson C., Davies R.D., Davis R.J., Gorski K.M., 2003, MNRAS, 345, 897
- Bennett C.L. et al., 2003a, ApJS, 148, 1
- Bennett C.L. et al., 2003b, ApJ, 148, 97
- Bernardi G., Carretti E., Fabbri R., Sbarra C., Poppi S., Cortiglioni S., 2003a, MNRAS, 344, 347
- Bernardi G., Carretti E., Cortiglioni S., Sault, R.J., Kesteven M.J., Poppi S., 2003b, ApJ, 594, 5
- Baccigalupi C., Burigana C., Perrotta F., De Zotti G., La Porta L., Maino D., Maris M., Paladini R., 2001, A&A, 372, 8
- Brouw W.N., Spoelstra T.A.T. 1976, A&AS, 26, 129
- Bruscoli M., Tucci M., Natale V., Carretti E., Fabbri R., Sarra C., Cortiglioni S., 2002, NewA, 7, 171
- Cortiglioni et al., 2003, in 16<sup>th</sup> *ESA Symposium on European Rocket and Balloon Programmes and Related Research*, Ed. B. Warmbein, ESA Proc. SP-530, p. 271
- Cortiglioni et al., 2004, NewA, 9, 297
- Dodelson S., 1997, ApJ, 482, 577
- Draine B.T., Lazarian A., 1998, ApJL, 494, 19
- Duncan A.R., Haynes R.F., Jones K.L., Stewart R.T., 1997, MNRAS, 291, 279
- Gaensler B.M., Dickey J.M., McClure-Griffiths N.M., Green A.J., Wieringa M.H., Haynes R.F., 2001, ApJ, 547, 41
- Giardino G., Banday A.J., Gorsky K.M., Bennet K., Jonas J.L., Tauber J.A., 2002, A&A, 387, 82
- Haslam C.G.T., Stoffel H., Salter C.J., Wilson W.E., 1982, A&AS, 47, 1
- Jonas J. L., Baart E. E., Nicolson, G. D., 1998, MNRAS, 297, 977
- Kamionkowski M., Kosowky A., 1998, PRD, 57, 685
- Kogut A., Hinshaw G., 2000, ApJ, 543, 530
- Kogut A., et al., 2003, ApJS, 148, 161
- Kovac J., Leitch E.M., Pryke C., Carlstrom J. E., Halverson N. W., Holzapfel W. L., 2002, Nat., 420, 772
- Lagache G., 2003, A&A, 405, 813
- Landecker T.L., Uyaniker B., Kothes R., 2002, in S. Cecchini, S. Cortiglioni, R. Sault, C. Sbarra, eds., AIP Conf. Proc. 609, Astrophysical Polarized Backgrounds, New York, p. 9

<sup>\*</sup> <http://www.eso.org/science/healpix/>

<sup>†</sup> <http://lambda.gsfc.nasa.gov/>

- de Oliveira Costa A., Tegmark M., Davies R.D., Gutierrez C.M., Lasenby A.N., Rebolo R., Watson R.A., 2003, *astro-ph/0312039*
- Platania P., Bensadoun M., Bersanelli M., De Amici G., Kogut A., Levin S., Maino D., Smooth G.F., 1998, *ApJ*, 505, 473
- Reich P., Reich W., 1988, *A&AS*, 74, 7
- Reich W., *A&A Suppl. Series*, 1982, 48, 219
- Sbarra C., Carretti E., Cortiglioni S., Zannoni M., Fabbri R., Macculi C., Tucci M., 2003, *A&A*, 401, 1215
- Sofue Y., Fujimoto M., 1983, *ApJ*, 265, 722
- Spergel D.N. et al., 2003, *ApJ*, 148, 175
- Tucci M., Carretti E., Cecchini S., Fabbri R., Orsini M., Pierpaoli E., 2000, *NewA*, 5, 181
- Zaldarriaga M., 1998, *ApJ*, 503, 1

This paper has been produced using the Royal Astronomical Society/Blackwell Science L<sup>A</sup>T<sub>E</sub>X style file.